A Mathematical Model of the Pancreatic Duct Cell Generating High Bicarbonate Concentrations in Pancreatic Juice

David C. Whitcomb, MD, PhD, and G. Bard Ermentrout, PhD†*

Objective: To develop a simple, physiologically based mathematical model of pancreatic duct cell secretion using experimentally derived parameters that generates pancreatic fluid bicarbonate concentrations of >140 mM after CFTR activation.

Methods: A new mathematical model was developed simulating a duct cell within a proximal pancreatic duct and included a sodium-2-bicarbonate cotransporter (NBC) and sodium-potassium pump (NaK pump) on a chloride-impermeable basolateral membrane, CFTR on the luminal membrane with 0.2 to 1 bicarbonate to chloride permeability ratio. Chloride-bicarbonate antiporters (Cl^-/HCO_3^- AP) were added or subtracted from the basolateral (AP_b) and luminal (AP_l) membranes. The model was integrated over time using XPPAUT.

Results: This model predicts robust, NaK pump–dependent bicarbonate secretion with opening of the CFTR, generates and maintains pancreatic fluid secretion with bicarbonate concentrations >140 mM, and returns to basal levels with CFTR closure. Limiting CFTR permeability to bicarbonate, as seen in some CFTR mutations, markedly inhibited pancreatic bicarbonate and fluid secretion.

Conclusions: A simple CFTR-dependent duct cell model can explain active, high-volume, high-concentration bicarbonate secretion in pancreatic juice that reproduces the experimental findings. This model may also provide insight into why CFTR mutations that predominantly affect bicarbonate permeability predispose to pancreatic dysfunction in humans.

Key Words: bicarbonate, chloride, pancreatitis, pancreas, secretin, sodium bicarbonate cotransporter (NBC), cystic fibrosis transmembrane conductance regulator (CFTR), antiporter, anion channel

(*Pancreas* 2004;29:e30–e40)

Received for publication January 20, 2004; accepted April 20, 2004.

From the *Departments of Medicine, Cell Biology and Physiology, and Human Genetics, University of Pittsburgh, Pittsburgh, Pennsylvania; and †Department of Mathematics, VA Pittsburgh Health Care System, Pittsburgh, Pennsylvania.

Presented in part at the XXXI Meeting of the European Pancreatic Club/Frontiers in Pancreatic Physiology Conference, Lüneberg, Germany, July 28–Aug 1, 1999, and the XXXIV Meeting of the European Pancreas Club, Heidelberg, Germany, June 20, 2002.

Reprints: David C. Whitcomb, MD, PhD, University of Pittsburgh, UPMC Presbyterian, Mezzanine Level, C Wing, 200 Lothrop Street, Pittsburgh, PA 15213 (e-mail: whitcomb@pitt.edu).

The human pancreas secretes an impressive amount of sodium bicarbonate–rich fluid with each meal. The majority of fluid and bicarbonate in pancreatic juice arises from the pancreatic duct cells even though they compose only about 5% of the pancreatic mass. Dysfunction of duct cell bicarbonate secretion, as seen with mutations with the cystic fibrosis transmembrane conductance regulator (CFTR) gene in cystic fibrosis, leads to severe dysfunction of the pancreatic duct cells and eventual destruction of the exocrine pancreas.[1–3]

Humans, guinea pig, and some other species (but not rat or mouse) generate bicarbonate concentrations exceeding 140 mM. To understand the mechanisms used by the pancreas to generate these high-bicarbonate concentrations, the various ion channels, transporters, and membrane characteristics of the pancreatic duct cell must be organized into functional models. In its most basic form, the model must explain (a) the mechanisms bringing bicarbonate into the duct cell, (b) the mechanisms transporting bicarbonate across the apical membrane into the lumen, (c) the conditions required to generate high bicarbonate concentrations in the pancreatic duct lumen, and (d) the role of the CFTR, which is the regulator of pancreatic bicarbonate secretion.

Earlier models envisioned de novo generation of bicarbonate from carbon dioxide and water inside the duct cells via carbonic anhydrase II (CAII), followed by bicarbonate secretion through a luminal chloride-bicarbonate antiporter (Cl^-/HCO_3^- AP_l).[4,5] In this model, CFTR primarily provides a mechanism for chloride efflux into the lumen to serve as a continual source of chloride for the Cl^-/HCO_3^- AP_l and to dissipate the excess intracellular chloride that would accumulate through this process.[4–6] However, this model fails to explain bicarbonate secretion in systems with minimal luminal chloride[7] or the mechanisms generating pancreatic juice with bicarbonate concentrations exceeding 70 mM.[5–8]

A newer and very complex mathematical model was recently proposed that requires at least 2 types of duct cells with different physiological characteristics that are organized in series.[6] The proximal duct cells are essentially the high volume, low bicarbonate generating cells of older models, while a novel distal duct cell is envisioned that can maintain a high

bicarbonate concentration gradient across the apical membrane.[6] However, it requires that the novel distal duct cell functions only with the CFTR closed (minimal chloride conductance) and generates minimal fluid and bicarbonate secretion (efflux). Furthermore, combining a high volume, low bicarbonate proximal duct cell with a low volume, high bicarbonate generating duct cell fails because adding a large volume of fluid with bicarbonate at 70 mM with a small volume of fluid at ~140 mM will not produce a final bicarbonate concentration of 140 mM.

We envisioned a new model with limited basolateral chloride permeability and significant CFTR permeability to bicarbonate that should generate high bicarbonate concentrations in the proximal pancreatic ducts where the luminal volume was small compared with duct cell volume[9] (Figs. 1 and 2). We based our model on the premise that, because the sum of the luminal chloride and bicarbonate concentrations remains constant, the only way to increase bicarbonate concentrations is to remove chloride from the system, by both blocking chloride influx through the basolateral membrane and by reducing intracellular and luminal chloride through active fluid secretion into the intestinal lumen.[9] Furthermore, since both chloride and bicarbonate can both cross the apical membrane by anion channels (eg, CFTR) and by anion exchangers (eg, the Cl^-/HCO_3^- AP), then during steady-state secretion, the distribution of chloride and bicarbonate would be governed by the constant field equation.[9] Thus, to achieve active bicarbonate secretion from duct cells by an electrochemical gradient, the final intracellular chloride must be lower, and the steady-state membrane potential must be higher than previously predicted.[8]

In the present paper, we tested our hypotheses using a mathematical model of the duct cell placed within the anatomic constraints of proximal pancreatic ducts. Using the known biophysical[6] and anatomic constraints of the pancreas, we found that a single type of proximal pancreatic duct cell with a limited number of ion channels and a sodium-potassium pump (NK-ATPase) explains pancreatic bicarbonate secretion with pancreatic juice bicarbonate concentrations exceeding 140 mM. Furthermore, in this model bicarbonate secretion is initiated and maintained with opening of the CFTR and terminated with closure of the CFTR, allowing the system to return to basal conditions. Finally, this model provides a platform for studying the functional effects of various mutations that alter the biophysical properties of the major channels and ion transporters.

METHODS

Model Development

The primary elements of our duct cell model were built from experimentally derived evidence of ion channels, pumps, cotransporters, and antiporters as summarized by Sohma et al,[6] with sodium bicarbonate cotransporter (NBC) coupling ratio of 1:2.[10] The initial mathematical model was based on the proximal rat duct cell model of Sohma et al.[6] The anatomic constraints were based on the histologic appearance of the pancreas, in which the duct cell volume to lumen volume is high. This is illustrated in Figure 1. The luminal compartment is open to fluid and electrolyte loss at the distal end of the duct, which leads to the intestine. The model is illustrated in Figure 2 and includes the acinus with attached duct plus (Fig. 2A) an exploded view of a duct cell and lumen illustrating the organization of the major channels, pumps, and exchanges (Fig. 2B).

Mathematical Modeling

The complete duct cell model consists of 3 compartments: the plasma compartment, the duct cell compartment, and the luminal compartment. The plasma compartment and duct cell compartments are separated by the basolateral (plasma) membrane and the duct cell compartment and luminal compartment are separated by the apical (luminal) membrane. Since the electrical potential difference (PD) between the lumen and the basolateral compartments is small (~1 mV),[5] we have short-circuited these 2 compartments, leaving only the potential difference between the cell and the plasma as the

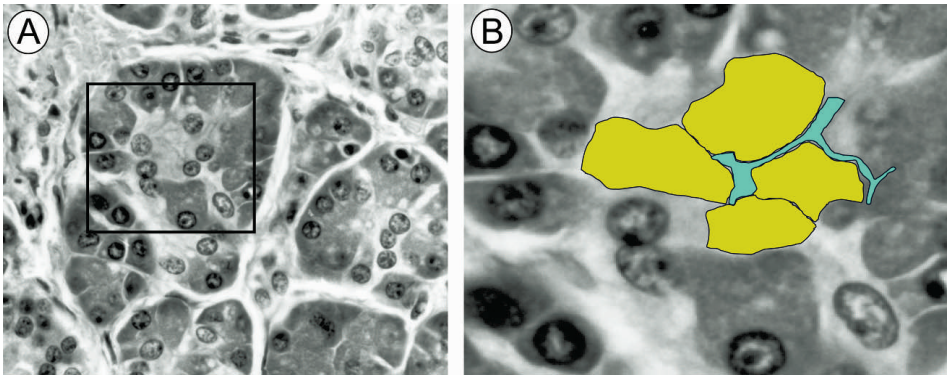

FIGURE 1. Photomicrograph of a pancreatic acini and proximal duct. A, The acinus is organized as a blind pouch with acinar cells forming the envelope and centroacinar cells forming the most proximal aspects of the pancreatic duct. B, Exploded section of A. Note the cross-sectional area of the centroacinar and proximal duct cells (yellow) versus proximal duct (blue).

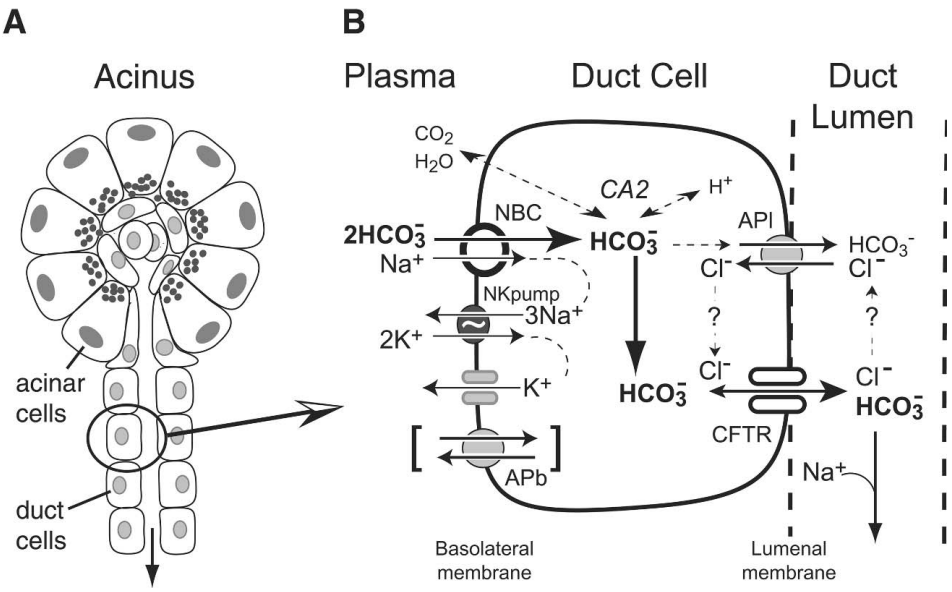

FIGURE 2. Structural organization of the duct cell model. A, Organization of the acinus with the acinar cells forming a cul de sac and with the duct cells, which extend into the acini as centroacinar cells, forming a conduit for the flow of secreted fluid. B, Model of the duct cell used in the complete model. For abbreviations, see text. The symbol AP_b indicates the location of the chloride/bicarbonate antiporter on the basolateral membrane that is inactivated in the standard model. The ? marks the sites of the hypothetical circulation of chloride out of CFTR and in through the AP_l in exchange of bicarbonate during active secretion in previous models that is not active or necessary in the current complete model under standard conditions.

voltage variable. In the simplest version of the model, we track only the transmembrane PD and the bicarbonate and chloride concentrations inside the cell and in the lumen. This is done by clamping the intracellular sodium. In a more complicated version of the model, we incorporate a simplified version of the sodium-potassium pump, which can then be disabled, allowing for sodium accumulation in the cell through the NBC. We also added a small sodium leak but not the sodium-hydrogen exchanger. In the lumen, we have a constant source of bicarbonate and chloride originating from the acinar cells at ion concentrations equivalent to plasma. Additionally, a flow out of the lumen is included that maintains both constant volume and constant ionic strength. When anions (chloride and bicarbonate) enter the lumen from the duct cell, they are modeled to cause an influx of water (via osmosis) and cations (eg, sodium) with proportional secretion of an ion-containing fluid out of the duct lumen (toward the intestine) so that the overall ion concentration in the lumen remains constant while the volume and secretion change in proportion to duct cell ion efflux. The apical (luminal) cell membrane contains a Cl^-/HCO_3^- AP and the CFTR channel (Fig. 2). The basolateral cell membrane contains the NBC and another Cl^-/HCO_3^- AP that is disabled during active secretion in the final model.[11] Inside the cell are buffers (eg, CAII) that maintain the intracellular bicarbonate concentration within a physiological range.

The CFTR channel should be modeled by the constant field equation. However, we simplify this by linearizing about the reversal potential to obtain a current that is linear in the potential. We apply the same ideas to the NBC channel, which is also voltage dependent. This allows us to solve for the steady-state voltage, further simplifying the equations. As one more simplification, we note that osmotic balance requires that the total luminal chloride and bicarbonate must be around 160 mM. Thus, we can eliminate the equation for the change in luminal chloride concentration; it must follow the luminal bicarbonate concentration.

Thus, there are only 4 differential equations for the normal system: intracellular bicarbonate, luminal bicarbonate, intracellular chloride, and intracellular sodium. The model can be further simplified if we clamp the intracellular sodium and bicarbonate. The resulting system is 2-dimensional and can be readily analyzed. However, that is beyond the scope of the present paper. The necessary channels, exchangers, and pumps were modeled as follows:

Antiporter

We use the equations for luminal Cl^-/HCO_3^- AP flux according to Sohma et al[6]:

$$J_{apl} = g_{apl} \frac{c_l b_i - b_l c_i}{k_c k_b [(1 + c_i/k_c + b_i/k_b)(c_l/k_c + b_l/k_b) + (1 + c_l/k_c + b_l/k_b)(c_i/k_c + b_i/k_b)} \quad (1)$$

where $k_b = 1$, $k_c = 10$, and b_i, b_l are bicarbonate concentrations and c_i, c_l are chloride concentrations. The subscripts *i* and *l* are intracellular and luminal values, respectively. The basolateral antiporter flux J_{apbl} is defined similarly.

CFTR

We use the constant field equation and then linearize around the equilibrium potential. We first define an effective permeability (the coefficient found by linearizing the constant field equation around the equilibrium potential):

$$g(x_i, x_o) = x_i x_o \ln(x_i/x_o)/(x_i - x_o) \quad (2)$$

where x_I, x_o are concentrations inside and outside the cell. Thus, the effective conductance of the channel is given by:

$$g_{cftr,c} = \bar{g}_{cftr,c} g(c_i, c_l) \tag{3}$$

$$g_{cftr,b} = \bar{g}_{cftr,b} g(b_i, b_l) \tag{4}$$

We generally set $\bar{g}_{cftr,b}/\bar{g}_{cftr,c} = 0.2$,[12] and defined this ratio as ρ, although experimentally derived ratios may vary depending on the species, the direction of ion flow,[13] or intracellular regulatory factors.[14] Thus, the fluxes are

$$J_{cftr,b} = g_{cftr,b}(V - E_b) \tag{5}$$

$$J_{cftr,c} = g_{cftr,c}(V - E_c) \tag{6}$$

$$E_b = \frac{RT}{F} \ln \frac{b_i}{b_l} \tag{7}$$

$$E_c = \frac{RT}{F} \ln \frac{c_i}{c_l} \tag{8}$$

The latter 2 quantities are the Nernst potentials for bicarbonate and chloride, respectively.

NBC

NBC is an electrogenic transporter, and the model used in Sohma et al[6] is quite complex. We have opted for a very simple linear model of the NBC (equations 9 and 10) with a 1:2 sodium to bicarbonate transport ratio[10]:

$$J_{nbc} = g_{nbc}(V - E_{nbc}) \tag{9}$$

where

$$E_{nbc} = \frac{RT}{F} \ln \frac{b_i^2 n_i}{b_p^2 n_p} \tag{10}$$

is the reversal potential. Here b_p,n_p are the plasma bicarbonate and sodium concentrations and n_i is the intracellular sodium concentration.

Sodium/Potassium Pump

The N^+/K^+ pump was modeled as:

$$J_{\text{nakpump}} = g_{\text{nak}} (V - E_{nak}) (n_i/n_{i0})^3 \tag{11}$$

where n_{i0} is the saturation constant for sodium. This is a simplified version of the model in Sohma et al.[6] Since potassium is clamped in our model, we absorb its dependence into the constant g_{nak}.

Luminal Flux

The ion and fluid flux out of the lumen represents secretion and is computed as follows. There is a small constant source of bicarbonate and chloride flux into the lumen from the acinar cells. Additionally, there is flux of both ions from the cell across the apical membrane. Thus, the total ionic flux is

$$J_{lumen} = J_{c,l} + J_{b,l} \tag{12}$$

$$J_{c,l} = J_{ac} + (J_{apl} - J_{cftr,c}) V_r \tag{13}$$

$$J_{b,l} = J_{ac} r + (J_{apl} - J_{cftr,c}) V_r \tag{14}$$

Note the last 2 quantities are the influx of the 2 ions into the lumen, $r = 0.25$ is the molar ratio of bicarbonate to chloride in the acinar cell source, and V_r is the volume ratio of the cell to the lumen and was set to 10. Luminal bicarbonate and chloride are carried out of the lumen at a rate proportional to their concentrations and J_{lumen}. The proportionality constant is chosen so that the total concentration of bicarbonate and chloride in the lumen is 160 mM.

Cellular Fluxes

The fluxes within the cell are

$$J_{c,i} = J_{cgftr,c} - J_{abl} - J_{apbl} \tag{15}$$

$$J_{b,i} = J_{cftr,b} + J_{apl} + J_{apbl} + 2J_{nbc} + \beta(b_{i0} - b_i) \tag{16}$$

$$J_{n,i} = J_{nbc} - J_{nak} - J_{naleak} \tag{17}$$

The buffering of bicarbonate is a simple production and destruction term of bicarbonate and can be turned on or off with the parameter β. We have added a small sodium leak into the cell J_{naleak} to keep the sodium concentration inside the cell at about 14 mM at rest. The sodium leak was modeled as

$$J_{naleak} = g_{naleak} (V\text{-}E_{na}) \tag{18}$$

where

$$\mathrm{E_{na}} = (\mathrm{RT/F}) \ln (\mathrm{n_p/n_i}) \tag{19}$$

The N^+/K^+ pump and the sodium leak can then be turned off by setting $g_{nak} = g_{naleak} = 0$, thus allowing the intracellular sodium to be determined by NBC.

Potential

The potential is assumed to act quickly (the capacitance is small compared with the ionic currents) so that it reaches equilibrium. Since we have linearized the constant field equation, this means we can easily solve for the equilibrium potential:

$$V = \frac{g_{nbc}E_{nbc} + g_{cftr,b}E_b + g_{cftr,c}E_c + g_k E_k + g_{naleak}E_{naleak}}{g_{nbc} + g_{cftr,b} + g_{cftr,c} + g_k + g_{naleak}} \tag{20}$$

We include a small potassium conductance through the basolateral membrane to allow dissipation of potassium that accumulates as a function of the sodium-potassium pump, although this is not necessary.

Standard Concentrations

We used the following concentrations as resting values: $n_p = 140$, $n_i = 14$, $b_p = 25$, $b_i = 15$, $b_l = 32$, $c_p = 110$, $c_i = 60$,

$c_l = 128$. The subscript p means plasma. The temperature was taken to be 37°C.

With these definitions, we are now able to write the differential equations for the model. As we pointed out above, we have arranged the model so that the total luminal bicarbonate and chloride equal 160 mM; thus, an equation for c_l is unnecessary. The equations are

$$c_i' = \zeta J_{c,i} \tag{21}$$

$$b_l' = \zeta(J_{b,l} - J_{lumen} b_l) \tag{22}$$

$$b_i' = \zeta J_{b,i} \tag{23}$$

$$n_i' = \zeta J_{n,i} \tag{24}$$

The parameter ζ is equivalent to uniformly scaling all the conductances and permeabilities. It does not change their relative values (their ratios). Free parameters are the maximum permeabilities, conductances, and the flux of the acinar cells. Thus, ζ is a common factor to all of the equations. In the standard unstimulated model, $J_{ac} = 0.025$, $g_{nbc} = 1$, $g_{apl} = 0.2$, $g_{apbl} = 0$, $g_{nak} = 3.125$, $E_{nak} = -200$ mV and $n_{i0} = 25$ mM, $\beta = 0.1$, $\zeta = 0.05$, $b_{i0} = 15$, and $\lambda = 0$. We stimulate the system by turning on g_{cftr} to a value of 1. The code (Appendix) is integrated using the author's (G.B.E.) software program, XPPAUT (http://www.pitt.edu/~phase). The complete code file is available from the authors upon request.

RESULTS

Complete Duct Cell Model

The complete duct cell model was tested under a variety of conditions. Figure 3 illustrates the predictions of the final duct cell model. CFTR is opened at 1 minute (first arrow), remains open for 5 minutes, and then closed (second arrow) for the remaining 4 minutes. Note that during steady state (~1 minute after CFTR opening until CFTR closure). The luminal bicarbonate concentration is maintained at 143 mM (Fig. 3A). Under basal conditions (from 0 to 1 minute), all ions in the lumen (Fig. 3A) and all fluid secretion (Fig. 3C) originate from acinar cells. Note also that the membrane potential (V) (Fig. 3B) is about −75 mV, which is maintained by NBC (reversal potential about −89 mV; equation 10) and the sodium leak (equation 18). Finally, at rest, the net flux across luminal antiporter (J_{apl}) is 0, since (from equation 1) $c_l b_i = c_i b_l$.

Opening of the CFTR (Fig. 3, first arrow) resulted in rapid depolarization of the duct cell (Fig. 4, first arrow) followed by a partial repolarization that is maintained as long as CFTR is open. Duct cell depolarization also resulted in an influx of sodium and bicarbonate at the basolateral membrane through NBC (ie, an increase in J_{nbc} as a result of decreasing V; equation 9). Three distinct phases of depolarization are observed after opening of the CFTR (Figs. 3 and 4): a rapid depolarization phase mediated primarily by chloride efflux through CFTR (Fig. 3B), a transitional phase reflecting a loss

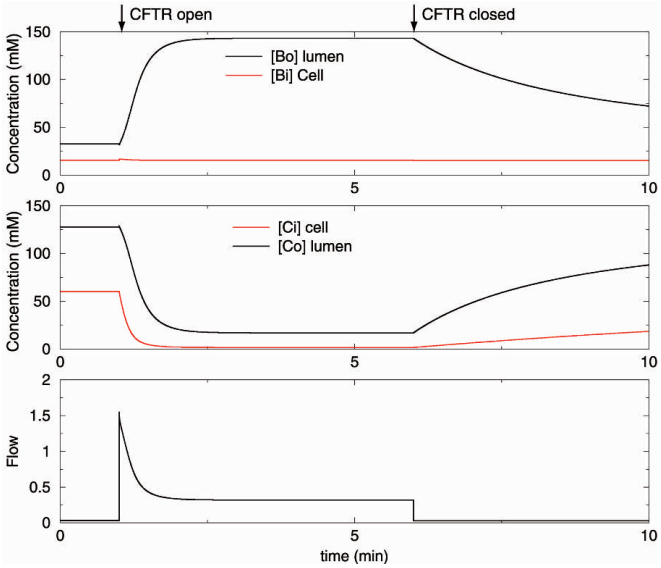

FIGURE 3. Anion concentrations and flow in the complete duct cell model as a function of CFTR. A, Concentrations of bicarbonate and chloride in the intracellular (i) and luminal (o) compartments as a function of time. Bicarbonate concentrations inside the duct cell (Bi) and in the lumen (Bo). The first arrow marks CFTR opening at 1 minute, the second arrow marks CFTR closing after 5 minutes (ie, at the 6-minute mark). Note that the luminal bicarbonate concentration quickly reaches the target concentration of >140 mM within about 1 minute under standard conditions. B, Chloride concentrations plotted as in A for bicarbonate. Note the relative low chloride concentrations inside the cell during active secretion. C, Flow of pancreatic juice in arbitrary units. The basal flow is due entirely to secretion of plasma-like fluid from the acinar cells. The fluid volume is closely associated with ion efflux from the duct cell (Fig. 4).

in intracellular chloride and a shift to bicarbonate secretion, and a steady-state potential reflecting an equilibrium between bicarbonate influx through the NBC and bicarbonate secretion through CFTR (equation 20). Note also that at steady state, the chloride concentrations in the cell relative to the lumen becomes dependent on the membrane potential, and chloride flux ($J_{cftr,c}$) becomes 0 when $V = E_c$ (equations 6 and 8). Thus, when potassium conductance is small, equation 20 can be simplified to

$$V = \frac{g_{nbc} E_{nbc} + g_{cftr,b} E_b}{g_{nbc} + g_{cftr,b}} \tag{25}$$

Unlike chloride, intracellular and plasma sodium and plasma bicarbonate concentrations remain constant, and the intracellular concentration of bicarbonate increases only slightly (to 19.3 mM), so E_{nbc} (equation 10) is nearly constant and E_b (equation 7) is primarily dependent on the luminal bicarbonate concentration. The maximum concentration of luminal bicarbonate is limited, however, and remains <160 mM because of

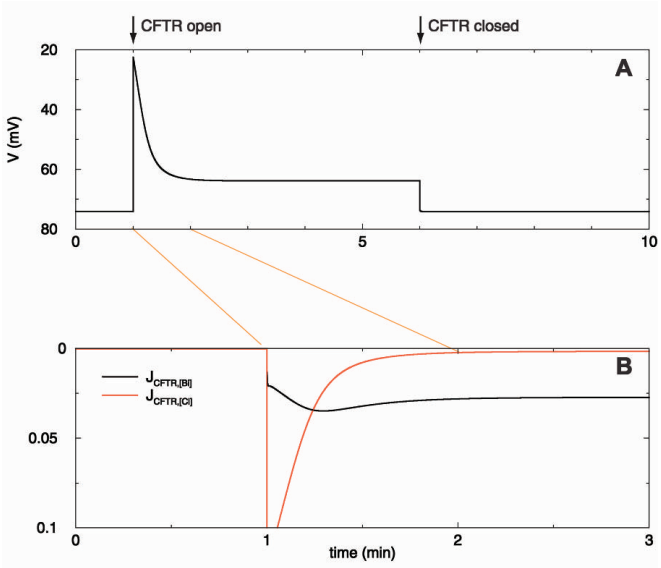

FIGURE 4. CFTR-dependent chloride and bicarbonate current. A, Current across the luminal membrane through CFTR. Note the tight linkage between anion-mediated current and through CFTR and pancreatic fluid secretion (Fig. 3C). B, Exploded view of A illustrating the components of the current mediated by chloride (red) and bicarbonate (black) during the first minute after CFTR opens.

osmosis and the resulting continual efflux of bicarbonate-rich fluid out of the pancreatic duct lumen and into the intestine at a rate equal to bicarbonate efflux from the duct cells (plus a small acinar cell component).

It can be seen from equation 25 that the steady-state membrane potential (V) will be somewhere between E_{nbc} and E_b and dependent on the relative permeability of NBC (g_{nbc}) and CFTR to bicarbonate ($g_{cftr,b}$). Note that initially g_{nbc} and g_{cftr} were equal (a value of 1), with g_{cftr} a function of $g_{cftr,c}$ and $g_{cftr,b}$. However, as chloride is lost and $g_{cftr,c}$ becomes irrelevant (ie, $E_c = V$ and $J_{cftr,c} = 0$; equation 6), $g_{cftr} \simeq g_{cftr,b}$ with $\rho = 0.2$ (equation 3). The membrane potential changes from about −22 mV when the CFTR first opened to about −64 mV at steady state, closer to reversal potential of NBC (Fig. 3B). This is a physiologically important observation because it allows bicarbonate to be secreted against a very high luminal bicarbonate concentration while maintaining an intracellular concentration of about 20 mM, which is linked to both pH and the partial pressure of CO_2 (Henderson-Hasselbalch relationship), which must be maintained within a physiological range. For bicarbonate to be secreted against a luminal concentration of 140 mM, it can be seen from equation 7 that V must be greater than about −53 mV, and this is achieved in the current model.

Changing the permeability of CFTR to chloride or bicarbonate, as seen with phosphorylation, ATP, and glutamate[14] or through select CFTR mutations,[14–16] has important consequences on duct cell function. In our model, reducing the permeability of CFTR to bicarbonate had profound effects on steady-state luminal bicarbonate concentrations (Fig. 5A), bicarbonate flux (Fig. 5C), and overall pancreatic fluid flow (Fig. 5B). Increasing $g_{CFTR,b}$ from 0.2 to 1 had little effect on further increasing the final bicarbonate concentration (Fig. 5A) but increased bicarbonate flux (Fig. 5C), which accounts for a proportional increase in pancreatic fluid flow (Fig. 5B). On the other hand, reducing the permeability of CFTR to chloride has little effect on bicarbonate secretion and fluid secretion in this model. Thus, pancreatic duct cell function is highly dependent on CFTR bicarbonate secretion but is relatively insensitive to changes only in chloride permeability.

Our model allows for the progressive loss of chloride from the duct cell and lumen through fluid secretion into the intestine. This results in depletion of chloride from the model with steady-state intracellular and extracellular chloride concentrations reaching 2 and 17 mM, respectively (Fig. 3A). If J_{ac} is reduced to 0 (equations 13 and 14), then the concentration of chloride in the cell and lumen approaches 0 and the luminal bicarbonate concentration reaches 160 mM (data not shown). When excess chloride is added to the lumen from the acinar cells by increasing J_{ac} from 0.025 to 0.1, the steady-state intracellular and extracellular chloride concentrations increase to 3.5 and 35.5 mM, respectively, with a drop in the luminal bicarbonate to 124.5 mM. These data and the sensitivity of the system to inward flux of chloride through APb (below) indicate that the model is very sensitive to addition of chloride from either the acinar cells or through the basolateral membrane of the duct cells.

Volume Ratios

One of the novel elements of our model is consideration of the anatomy of the acinus and proximal ducts.[9] The large cell:lumen volume ratios (V_r; equations 13 and 14) were predicted to cause rapid and significant changes of the luminal ion concentrations based on the type of anions entering the lumen from the acinar cells and duct cells that continually replace the previous ions that are then lost from the system due to secretion. We tested this hypothesis by evaluating V_r in our model at ratios of 1:10 to 1:1, 10:1 (standard), and 25:1, with J_{ac} linked to luminal volume (equations 13 and 14). Increasing the luminal volume resulted in progressively lower steady-state luminal bicarbonate concentration (Fig. 6). This situation reflects the more distal duct and suggests that effective bicarbonate secretion must occur at a proximal rather than distal site. When J_{ac} is kept constant, then maximal bicarbonate concentrations are eventually reached within the lumen with the time to steady state inversely proportional to V_r (data not shown). As the luminal volume approaches infinity, the effect of bicarbonate and/or chloride flux from the acinar cell on luminal bicarbonate concentration becomes minimal (equations 12–14).

The isolated duct cell represents a condition similar to a cell:lumen volume ratios of 1:infinity ($V_r \simeq 0$). In the complete

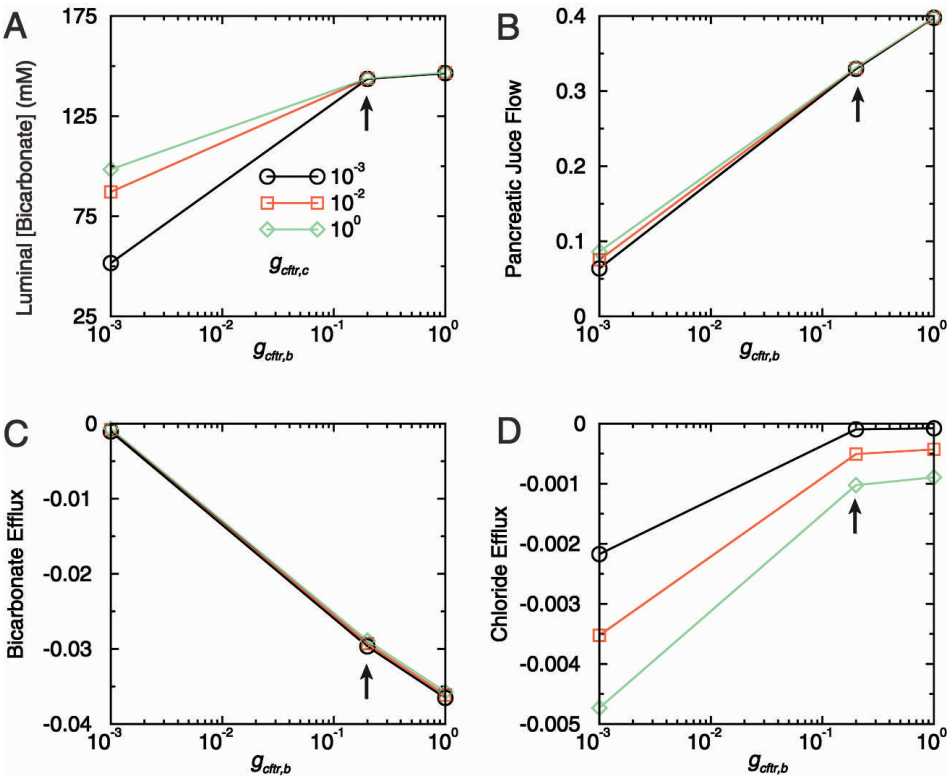

FIGURE 5. Effect of altering the permeability of bicarbonate or chloride through CFTR. The relative permeability of bicarbonate compared with chloride (ρ) was tested in the complete duct cell model. The horizontal axis in each panel is the strength of $g_{CFTR,Bi}$ relative to the normal permeability of CFTR in the open state to chloride, which is 1. The $g_{CFTR,Bi}$ was set at 0.001, 0.2 (standard model), and 1 in each panel. Each panel has 3 curves corresponding to $g_{CFTR,Cl}$ of 0.001 (black), 0.01 (red), and 1 (green, standard model). The arrow marks the standard conditions. A, Steady-state luminal bicarbonate concentration as a function of $g_{CFTR,Bi}$ and $g_{CFTR,Cl}$. Note that the steady-state luminal bicarbonate concentration is maintained above 140 mM regardless of CFTR chloride permeability until $g_{CFTR,Bi}$ drops below 0.2. B, The flow of pancreatic juice during steady-state secretion is dependent on bicarbonate rather than chloride permeability. C, Bicarbonate flux out of the duct cell (therefore a negative value) is only dependent on bicarbonate permeability. D, Chloride flux is dependent on both chloride and bicarbonate permeability (note also the different scale in C vs. D).

model, setting V_r to 0 results in a steady-state membrane potential of −45 mV and no net chloride flux [$J_{cftr,c} = \sim 0$, $V = E_c$; equation 8 (see also ref. 17)], yet with a positive bicarbonate efflux. Although this condition does not result in high bicarbonate concentrations, this process may be physiologically relevant in a variety of CFTR containing bicarbonate-secreting epithelial cells, since it is the quantity of bicarbonate secreted rather than the concentration that is important for neutralizing acids.

Chloride-Bicarbonate Antiporters

This model allows us to determine the effect of adding or subtracting the Cl^-/HCO_3^- APs to the luminal or basolateral membrane of the duct cell by multiplying g_{apl} or g_{apb} by 1 (on) or 0.005 (off). Figure 7 illustrates the effect of having only the luminal antiporter (AP_l) *on*, as in the complete duct cell model (Fig. 5A), both AP_l and the basolateral antiporter (AP_b) *off* (Fig. 5B), and AP_l and AP_b *on* (Fig. 5C). These simulations indicate that active secretion does *not* require AP_l (Fig. 5B). Comparing Figure 5A and B reveals a slightly higher extracellular bicarbonate level in the absence of AP_l. This indicates that, at steady state, the direction of ion flow through the antiporter is bicarbonate *in* for chloride *out*, the exact opposite direction of exchange envisioned by earlier models (Fig. 2B). Although AP_l has little effect on active secretion, it is important *after* CFTR is closed to allow intracellular chloride concentrations to return to basal values (Fig. 7B). The addition of AP_b, as required in other models,[6] provides a constant source of chloride from the plasma through the basolateral membrane and prevents the duct cell from generating high bicarbonate concentrations (Fig. 5C). However, AP_b, like AP_l, is effective in reestablishing basal intracellular chloride levels after CFTR is closed. Additional CFTR-linked anion antiporters with unidirectional and/or electrogenic properties may also exist, but they were not modeled here.

Na^+K^+ Pump

The model also predicts that the driving force for bicarbonate secretion is the basolateral Na^+/K^+ pump. When the Na^+/K^+ pump is turned off by setting g_{nk} to 0, the intracellular sodium concentrations rise to 80 mM and the reversal potential of the NBC falls to −35 mV (equation 10), the membrane potential goes to −30 mV and bicarbonate secretion essentially stops (not shown).

CAII

In the absence of duct cell CAII, the intracellular bicarbonate concentration rapidly rises to >40 mM during the rapid

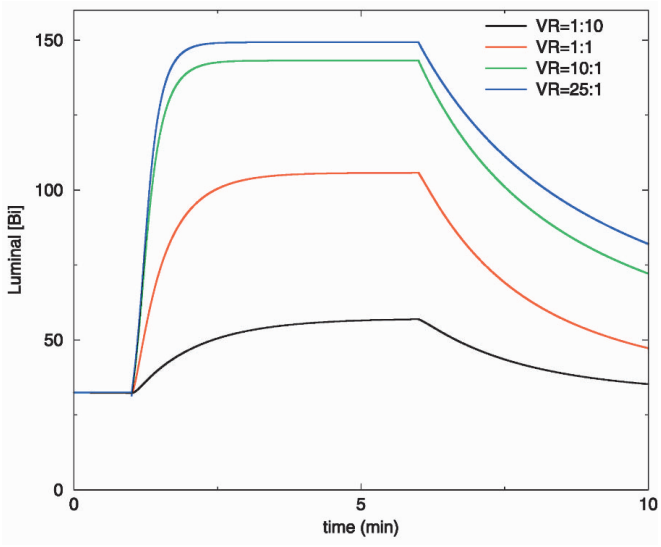

FIGURE 6. Effect of different duct cell volume to lumen volume ratios on steady-state bicarbonate final concentration. The ratio between duct cell volume and luminal volume was tested at 1:10 to 1:1, 10:1(standard), and 25:1 in the complete model. Note the progressive reduction in the maximum bicarbonate concentration under the experimental conditions (eg, acinar cell fluid flow kept proportional to luminal volume).

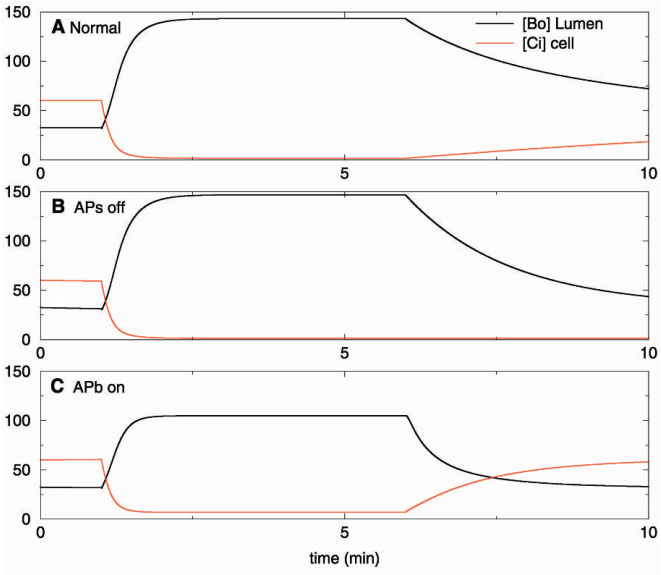

FIGURE 7. Effects of the APs on luminal bicarbonate concentration. A, Complete model with APl on and APb off. B, Duct model with both APs off. Note that absence of the APl has no effect on the generation or maintenance of high luminal bicarbonate concentration but eliminates recovery of the duct cell after CFTR closure since there is no other pathway of chloride entry into the duct cell. C, Duct model with both APs on. In this model, there is a continuous source of chloride to the duct cells so that both chloride and bicarbonate are secreted. Note that the final concentration of bicarbonate in the lumen is markedly reduced compared with that in the complete model (A) or without antiporters (B).

depolarization phase (not shown). Inclusion of CAII to the duct cell prevented the rise of intracellular bicarbonate above ~20 mM yet has no effect on overall bicarbonate secretion. Thus, in this model, the CAII appears to act as a buffer.

DISCUSSION

The mechanisms used by the pancreas to generate very high bicarbonate concentrations have been elusive. The reasons for this include the technical difficulty in obtaining, maintaining, and investigating proximal pancreatic duct cells, the difference in duct cell physiology between species, limited attention to the anatomic organization of the duct cells within the proximal pancreatic ducts, and lack of information on the biophysical properties of CFTR, NBC, and other ion regulators. The use of mathematical modeling and computer simulations provides a useful way to test some basic hypotheses that challenge the limits of current experimental techniques.

The central requirement of any pancreatic duct cell model is transport of bicarbonate against a significant concentration gradient into a high bicarbonate solution.[9] Early duct cell models envisioned CFTR as a chloride channel that was functionally linked to the Cl^-/HCO_3^- AP_l (Fig. 2B, "?"). CFTR supplied luminal chloride to exchange for intracellular bicarbonate, though Cl^-/HCO_3^- AP_l, and prevent the intracellular accumulation of chloride from entering the duct cell in exchange for bicarbonate.[4] However, the discovery that most of the secreted bicarbonate enters the duct cell via an electrogenic, basolateral NBC[8,18–20] and the demonstration that AU2 CFTR activation alters membrane potential suggested that CFTR's role was to depolarize the duct cell and thereby facilitate bicarbonate influx via the NBC.[20,21]

Our model added at least 2 critical conceptual changes to previous models of bicarbonate-secreting pancreatic duct cells. The first is the nearly complete elimination of chloride from the system (requiring a low steady-state intracellular chloride concentration), which is accomplished with a chloride-impermeable basolateral membrane and an anatomically small lumen[9] (Fig. 1). This would logically occur in the proximal duct, which also appears to be the primary site of bicarbonate production in the pancreas based on the localization of CFTR,[22] NBC,[23] and the NaK ATPase pump[23] (cf Marino et al[23]; Fig. 3E,F). The cul-de-sac organization of the proximal duct within the acinus also facilitates the unidirectional secretory flow and chloride ion washout.[9] The removal of significant chloride and electrochemical equilibration of chloride across the membrane allows CFTR to facilitate bicarbonate conductance without net chloride flux, even though CFTR remains more permeable to chloride than bicarbonate. The second conceptual change is using the electrochemical gradient of

bicarbonate across a bicarbonate permeable luminal membrane to drive bicarbonate secretion without employing antiporters, cotransporters, or pumps. This is consistent with the observations that the basolateral NaK pump appears to drive bicarbonate secretion,[4] and, to our knowledge, no other bicarbonate-linked pump has been identified. Furthermore, if CFTR was permeable to bicarbonate, then the Cl^-/HCO_3^- AP_l may be unnecessary for the bulk of bicarbonate efflux, especially since ion flux is usually several orders of magnitude greater through channels than through antiporters. Furthermore, we could not conceive of a steady-state electrical or chemical gradient combination in the duct cell that could drive chloride in both directions at the same time, ie, out through CFTR and *in* through AP_l in exchange for bicarbonate, with the end result of low luminal chloride and high luminal concentrations.

If a major bicarbonate-permeable anion channel (eg, CFTR) remains open during active bicarbonate secretion, we argued that the driving force for bicarbonate secretion would be determined by the electrochemical gradient.[9] The direction of bicarbonate flux across a permeable luminal membrane can be predicted by the Nernst equation (eg, equation 7). For example, at a temperature of 300°K, an intracellular bicarbonate concentration of 16 mM, and an extracellular bicarbonate concentration of 140 mM, the reversal potential will be −56 mV. Thus, if the membrane potential is more negative than −56 mV, bicarbonate would be driven out of the cell, whereas at membrane potentials less than −56 mV, bicarbonate flux would be into the cell. From this we conclude that during active bicarbonate secretion, the membrane PD of the duct cell must be greater than −56 mV (in contrast to the −30 mV measured in earlier experiments). However, if CFTR were indeed the dominant anion channel, then chloride, as a monovalent anion, would be influenced by the same electrical field as bicarbonate. If the luminal chloride concentration were 18 mM, for example, the intracellular chloride concentration at steady state would be about 2 mM (Fig. 3A). Interestingly, more recent experiments in isolated pancreatic ducts from guinea pigs (which secrete fluid with high bicarbonate concentrations) are confirming our earlier predictions of a membrane potential of more than −56 mV and low intracellular chloride concentrations during active secretion.[7,24]

CFTR is critical to pancreatic duct cell function including normal bicarbonate secretion.[2] CFTR is clearly an anion channel that is also permeable to bicarbonate with experimentally measured HCO_3^- to Cl^- permeability ratios ranging from 0.5:1 to 0.02:1 in most high bicarbonate–secreting species investigated.[13,25,26] The maintenance and regulation of CFTR chloride and bicarbonate permeability appear to have significant physiologic implications. Choi et al[15] studied a series of human CFTR mutations that retained substantial or normal chloride channel activity but had significantly reduced bicarbonate permeability. They found that CFTR mutations associated with cystic fibrosis and pancreatic insufficiency often had reduced bicarbonate permeability to levels <10% of normal, without changes in chloride permeability. However, CFTR mutations associated with cystic fibrosis and pancreatic sufficiency had bicarbonate transport ratios 31% and 46% of the normal ratio. This research group subsequently suggested that these findings might be explained by other CFTR-regulated bicarbonate transporters (eg, SLC26) in the event that CFTR was impermeable to bicarbonate.[16] However, much of the work on these transporters is done in mice or rats, which do not secrete high bicarbonate concentrations in pancreatic juice. Thus, these rodents may not be the best models for the study of all elements of human duct cell physiology. In support of the bicarbonate-permeable CFTR model is recent work by Reddy and Quinton,[14] who demonstrated that CFTR was not only permeable to bicarbonate but that that control of CFTR permeability to chloride and bicarbonate was both selective and dynamic (eg, cells can selectively increase CFTR bicarbonate permeability).

CFTR mutations located in the nucleotide binding domain (NBD-1) are often associated with defective channel regulation and gating and result in cystic fibrosis with pancreatic insufficiency. According to Reddy and Quinton,[14] NBD-1 regulates bicarbonate secretion and disruption of these sites is likely responsible for the more severe forms of cystic fibrosis. This observation is highly relevant to our duct cell model because selective impairment of CFTR-mediated bicarbonate conductance would functionally eliminate secretion in the pancreatic ductal epithelial cells, ie, chloride could not enter the cells and bicarbonate could not exit, resulting in minimal transcellular ion flux and minimal secretion. This point is illustrated in Figure 5, which predicts that the CFTR mutations that reduce bicarbonate permeability would impair pancreatic function, whereas mutations that alter only chloride permeability [eg, mutations in the CFTR regulatory (R) region[14]] would have little effect on pancreatic function.

In conclusion, we developed a mathematical model of the pancreatic duct cell using experimentally established parameters that demonstrate a mechanisms for secreting pancreatic juice with bicarbonate concentrations exceeding 140 mM that is turned on and off by CFTR. This model suggests that (a) bicarbonate is brought into the cell when linked to the sodium electrochemical gradient by NBC, (b) bicarbonate exits the cell into the lumen through an anion channel (probably CFTR), (c) the efflux is driven by the electrochemical gradient, and (d) CFTR serves to both depolarize the duct cell upon stimulation and facilitate bicarbonate efflux. Antiporters appear to be most important in the unstimulated state (CFTR closed) and may have a role in chloride-secreting species and conditions. Other channels or exchangers could be added but are not needed to reproduce the function of CFTR. This model also suggests that pancreas bicarbonate secretion at high concentrations is very sensitive to chloride from either the basolateral membrane or

acinar cells. These factors may explain some of the species differences in final pancreatic bicarbonate concentrations.

ACKNOWLEDGMENT

The authors are indebted to Robert Bridges, PhD, for critically reviewing this manuscript.

APPENDIX

Basic Pancreatic Duct Cell Model Code runs on XPPAUT. The complete code file for XPPAUT is available from the author (G.B.D.) upon request (bard@euler.math.pitt.edu) and through http://www.pitt.edu/~phase.

```
# bicarb9.ode
par g_bi=.2,g_cl=1
# overall factor to get the time scale right - multiplies all the
# permeabilities
par zeta=.05
# antiporter equation
ap(ao,ai,bo,bi,ka,kb)=(ao*bi-bo*ai)/(ka*kb*((1+ai/ka
+bi/kb)*(ao/ka+bo/kb)+(1+ao/ka+bo/kb)*(ai/ka+bi/kb)))
# parameters for the Bi/Cl antiporters
par kbi=1,kcl=10
# effective permeability due to linearizing the const
field eqn
g(xi,xo)=xi*xo*log(xi/xo)/(xi-xo)
# various conductances
par gnbc=2,gapl=.25,gapbl=0.005
# basolateral concentrations
par nb=140,bb=22,cb=130
# in case we want to turn off Na/K pump − intracellular
sodium can change
init ni=14
# volume ratio - 10:1, rho is Cl:Bi permeability
# buf is buffer
par vr=.1,bi0=15,buf=0.1,chi=1
# initial intracellular bicarb
init bi=15
# initial intracellular chloride, luminal bicarbonate
init ci=60,bl=32
# osmotic balance − force luminal chloride +
bicarbonate = 160 mM
cl=160-bl
par gcftron=1,
par gcftrbase=7e-5
par ek=−.085,gk=1
# membrane capacitance
par cap = 1
# physical constants
number r=8.31451,f=96485,temp = 310
# Nernst potential
eb=(r*temp/f)*log(bi/bl)
enbc=(r*temp/f)*log(bi^2*ni/(bb^2*nb))
ec=(r*temp/f)*log(ci/cl)
ena=(r*temp/f)*log(nb/ni)
# effective CFTR permeabilities
kccf=g(ci,cl)*gcftr*g_cl
kbcf=g(bi,bl)*gcftr*g_bi
knbc=gnbc
# potential is slaved to the concentrations
v = (knbc*enbc+kbcf*eb+kccf*ec+gk*ek+gnaleak*
ena)/(knbc+kbcf+kccf+gk)
# Active voltage-dependent fluxes
jnbc=knbc*(v-enbc)
jbcftr=kbcf*(v-eb)
jccftr=kccf*(v-ec)
# antiporters
japl=ap(bl,bi,cl,ci,kbi,kcl)*gapl
japbl=ap(bb,bi,cb,ci,kbi,kcl)*gapbl
# total ionic fluxes
jbl=(-jbcftr-japl)/vr+jac*rat
jci=jccftr-japl-japbl
jcl=(-jccftr+japl)/vr+jac
# ionic strength
par ionstr=160
# total scaled luminal flux
jlum=(jcl+jbl)/ionstr
jnak=gnak*(v-epump)*(ni/np0)^3
par gnak=3.125,np0=25,epump=−.2
jnaleak=gnaleak*(v-ena)
par gnaleak=.4
# flow
aux flow=jlum*ionstr
# acinar parameters - maintain 4:1 ratio of Cl:Bi at rest
par jac=.025,rat=.25
# differential equations for the concentrations
ci′=jci*zeta
bl′=(jbl-jlum*bl)*zeta
bi′=zeta*chi*(jbcftr+japl+japbl+buf*(bi0-bi)+2*jnbc)
ni′=zeta*(jnbc-jnak-jnaleak)
gcftr′=0
global 0 t {gcftr=gcftrbase}
global 1 t-ton*60000 {gcftr=gcftron}
global 1 t-toff*60000 {gcftr=gcftrbase}
par ton=1
par toff=6
# stuff to plot
aux enbc_=enbc
aux eb_=eb
aux ec_=ec
aux jnbc_=jnbc
aux jnac_=jnak
aux jbcftr_=jbcftr
aux jccftr_=jccftr
aux v_=v*1000
aux japl_=japl
```

```
aux japbl_=japbl
aux tt=t/60000
aux cl_=cl
# parameters for integration
@ xp=tt,yp=bl,xlo=0,xhi=12,ylo=0,yhi=150
@ nplots=3,yp2=ci,xp2=tt,yp3=bi,xp3=tt
@ bound=1000,total=660000,dt=50,meth=cvode
done
```

REFERENCES

1. Kerem B, Rommens JM, Buchanan JA, et al. Identification of the cystic fibrosis gene: genetic analysis. *Science*. 1989;245:1073–1080.
2. Drumm ML, Pope HA, Cliff WH, et al. Correction of the cystic fibrosis defect in vitro by retrovirus-mediated gene transfer. *Cell*. 1990;62:1227–1233.
3. Whitcomb DC. Hereditary and childhood disorders of the pancreas, including cystic fibrosis. In: Feldman M, Friedman LS, Sleisenger MH, eds. *Sleisenger and Fordtran's Gastrointestinal and Liver Disease*, 7th ed. Philadelphia: WB Saunders; 2002:881–904.
4. Case RM, Argent BE. Pancreatic duct cell secretion. Control and mechanism of transport. In: Go VLW, et al. eds. *The Pancreas: Biology, Pathobiology and Disease*, 2nd ed. New York: Raven Press; 1993:301–350.
5. Sohma Y, Gray MA, Imai Y, et al. A mathematical model of the pancreatic ductal epithelium. *J Membr Biol*. 1996;154:53–67.
6. Sohma Y, Gray MA, Imai Y, et al. HCO3 transport in a mathematical model of the pancreatic ductal epithelium. *J Membrane Biol*. 2000;176:77–100.
7. Ishiguro H, Steward MC, Wilson RW, et al. Bicarbonate secretion in interlobular ducts from guinea-pig pancreas. *J Physiol (Lond)*. 1996;495:179–191.
8. Ishiguro H, Steward MC, Lindsay AR, et al. Accumulation of intracellular HCO3- by Na(+)-HCO3- cotransport in interlobular ducts from guinea-pig pancreas. *J Physiol (Lond)*. 1996;495:169–178.
9. Whitcomb DC. Pancreatic bicarbonate secretion: the role of CFTR and the sodium-bicarbonate cotransporter. *Gastroenterology*. 1999;117:275–277.
10. Gross E, Abuladze N, Pushkin A, et al. The stoichiometry of the electrogenic sodium bicarbonate cotransporter pNBC1 in mouse pancreatic duct cells is 2 HCO3-:1 Na+. *J Physiol (Lond)*. 2001;531:375–382.
11. Ishiguro H, Naruse S, San Roman JI, et al. Pancreatic ductal bicarbonate secretion: past, present and future. *JOP*. 2001;2(suppl):192–197.
12. Gray MA, Pollard CE, Harris A, et al. Anion selectivity and block of the small-conductance chloride channel on pancreatic duct cells. *Am J Physiol*. 1990;259:C752–C761.
13. Linsdell P, Tabcharani JA, Rommens JM, et al. Permeability of wild-type and mutant cystic fibrosis transmembrane conductance regulator chloride channels to polyatomic anions. *J Gen Physiol*. 1997;110:355–364.
14. Reddy MM, Quinton PM. Control of dynamic CFTR selectivity by glutamate and ATP in epithelial cells. *Nature*. 2003;423:756–760.
15. Choi JY, Muallem D, Kiselyov K, et al. Aberrant CFTR-dependent HCO3- transport in mutations associated with cystic fibrosis. *Nature*. 2001;410:94–97.
16. Ko SB, Shcheynikov N, Choi JY, et al. A molecular mechanism for aberrant CFTR-dependent HCO(3)(-) transport in cystic fibrosis. *EMBO J*. 2002;21:5662–5672.
17. Devor DC, Singh AK, Lambert LC, et al. Bicarbonate and chloride secretion in Calu-3 human airway epithelial cells. *J Gen Physiol*. 1999;113:743–760.
18. Ishiguro H, Naruse S, Steward MC, et al. Fluid secretion in interlobular ducts isolated from guinea-pig pancreas. *J Physiol (Lond)*. 1998;511:407–422.
19. Burnham CE, Amlal H, Wang Z, et al. Cloning and functional expression of a human kidney Na+:HCO3- cotransporter. *J Biol Chem*. 1997;272:19111–19114.
20. Shumaker H, Amlal H, Frizzell R, et al. CFTR drives Na+-nHCO3 cotransporter in pancreatic duct cells: a possible basis for defective secretion in CF. *Am J Physiol*. 1999;276:C16–C25.
21. Stutts MJ, Gabriel E, Olseng JC, et al. Functional consequences of heterologous expression of the cystic fibrosis transmembrane conductance regulator in fibroblasts. *JBC*. 1993;268:20653–20658.
22. Marino CR, Matovcik LM, Gorelick FS, et al. Localization of the cystic fibrosis transmembrane conductance regulator in pancreas. *J Clin Invest*. 1991;88:712–716.
23. Marino CR, Jeanes V, Boron WF, et al. Expression and distribution of the Na(+)-HCO(-)(3) cotransporter in human pancreas. *Am J Physiol*. 1999;277:G487–G494.
24. Ishiguro H, Steward MC, Sohma Y, et al. Membrane potential and bicarbonate secretion in isolated interlobular ducts from guinea-pig pancreas. *J Gen Physiol*. 2002;120:617–628.
25. O'Reilly CM, Winpenny JP, Argent BE, et al. Cystic fibrosis transmembrane conductance regulator currents in guinea pig pancreatic duct cells: inhibition by bicarbonate ions. *Gastroenterology*. 2000;118:1187–1196.
26. Poulsen JH, Fischer H, Illek B, et al. Bicarbonate conductance and pH regulatory capability of cystic fibrosis transmembrane conductance regulator. *Proc Natl Acad Sci U S A*. 1994;91:5340–5344.